



# A Spraying Model of Non-atomizing Sprinkler based on Jet Fragmentation

L. Hua, H. Li<sup>†</sup> and Y. Jiang

*Research Center of Fluid Machinery Engineering and Technology, Jiangsu University, Zhenjiang 212013, Jiangsu, China*

<sup>†</sup>Corresponding Author Email: [hli@ujs.edu.cn](mailto:hli@ujs.edu.cn)

(Received December 15, 2021; accepted May 30, 2022)

## ABSTRACT

This work is devoted to the development of a new model for the non-atomizing sprinkler irrigation jet, for calculating the trajectories and landing positions of water droplets. The novelty of the proposed model is that the secondary breakup of the droplets can be calculated during the spraying process. For irrigation jet with a second wind-induced breakup regime, the model is optimized based on the ballistic theory by considering the secondary breakup of droplets and the jet breakup length. The wave-breaking model is used to determine the secondary breakup of the droplets. The output of this model is the water application rate that is calculated by using the cumulative volume of droplets along the radial spraying direction. A comparison of the results obtained using the proposed model with experimental data is conducted to verify the accuracy and reliability of the proposed model. The results show a good agreement of the peak water application rate between the optimized model and the experimental data, with an average error ranging within 6%. The droplets in the front spraying area usually have a diameter of 0-2 mm. This is computed by using the droplet secondary breakup sub-model, resulting in a considerably improved accuracy of the optimized model in the prediction of the water application rate of a sprinkler.

**Keywords:** Sprinkler irrigation; Droplets movement model; Ballistic theory; Secondary droplets breakup; Jet breakup length.

## NOMENCLATURE

$Re$	Reynolds number		drops of diameter less than $d$
$F$	inertial resistance	$n$	scatter coefficient
$A$	characteristic cross-section of the droplet of droplet	$\bar{d}$	average droplet diameter
$R$	radius of water droplet	$d_c$	characteristic droplet diameter
$\rho_w$	density of water	$d_{32}$	Sauter mean diameter
$\rho_a$	density of air	$d_e$	equivalent diameter
$g$	acceleration of gravity	$k_1$	correction coefficient of $d_c$
$C_d$	coefficient of air resistance	$k_2$	correction coefficient of $d_{32}$
$u_x$	velocity component in the $x$ direction	$We$	weber number
$u_y$	velocity component in the $y$ direction	$We_w$	weber number of water
$u_z$	velocity component in the $z$ direction	$We_a$	weber number of air
$V$	resultant velocity of droplets	$a$	scale parameter of the Gamma function
$L_b$	breakup length of jet	$b$	shape parameter of the Gamma function
$H$	pressure in meters of water	$V_0$	initial velocity of the water droplets
$D$	orifice diameter	$V_c$	critical velocity of the droplet secondary breakup
$d$	diameter of water droplets	$r$	radius of the sub droplet
$N$	number of water droplets	$R$	radius of the main droplet
$Q$	sprinkler flowrate	$B_1$	empirical coefficient
$X$	calculated flowrate	$\Delta t$	time step for calculation
$t$	spraying time	$I$	water application rate
$Y_d$	fraction of the total volume contained in	2DVD	Two-Dimensional Video Disdrometer

$\tau$	breaking time	$\nu$	dynamic viscosity of air
$\lambda$	wave length of the unstable waves	$\sigma$	surface tension coefficient of water
$\Omega$	maximum growth rate of the unstable waves	$\lambda$	radial integral length scale

## 1. INTRODUCTION

Sprinkler irrigation is a water-saving irrigation method that simulates the rainfall process to spread water on the crops and ground. During spraying, the water jet splits and breaks under the influence of external forces, and a group of water droplets with different diameters and velocities is formed possessing different trajectories. Finally, the water droplets cluster on different positions on the ground to form precipitation. To predict the droplet trajectory, various models have been established based on ballistic theory (Aghajani *et al.* 2014; Zhang *et al.* 2015). The accuracy of the spraying model is mainly affected by the initial conditions of the water droplets, including droplets diameter, initial position, and the air resistance on droplets during their movement through the air. However, these existing trajectory models are based on many simplified assumptions, which are not appropriate for modeling the spraying processes. Therefore, the use of these models for predicting the motion of droplets leads to inaccurate results.

The diameter of a water droplet affects its trajectory and landing position. According to the hydraulic configuration of agricultural sprinkler irrigation systems, the water droplets continuously fall from the jet along the ejection direction. The upper limit log normal model (Kincaid *et al.* 1996; Mugele and Evans 1951) effectively depicts the droplet diameter distribution. Li *et al.* (1994) proposed an exponential model that efficiently models the diameter distribution of the droplets, except for with the droplets whose diameters are smaller than 1 mm. However, the droplets' size distribution measured on the ground is different from that near the nozzle. Park and Wu (Park *et al.* 2005; Wu *et al.* 2020) discuss that the droplets of liquid jets near the nozzle conform to the Rosin-Rammler distribution. The water droplets formed by the breaking of jet vary considerably in terms of diameter, and some of them are called main droplets and the others are satellite droplets (Lin 1996; Munnannur and Reitz 2007). The large droplets are prone to asymmetric deformation, thus forming sub-droplets with a uniform diameter. This phenomenon is called secondary droplets breakup (Ashgriz and Poo 1990). A numerical simulation approach based on a wave breakup model assists in simulating the secondary breaking behavior of droplets (Liu *et al.* 1993). This allows to formulate a more accurate approach for modeling the trajectory of droplets that is more consistent with real sprinkler spraying.

As compared to the liquid jets atomizing into water droplets immediately at the orifice, the sprinkler irrigation jets have a continuous cylindrical water column before breaking into water droplets to obtain a larger wetting radius. This dense water column section is called the jet breakup length ( $L_b$ ).  $L_b$  is mainly related to the nozzle structure and jet velocity, which affects the initial position and state of the

water droplets produced during the primary jet breakup. Different values of  $L_b$  are used to determine the landing position of water droplets and the resulting wetting patterns (Jiang *et al.* 2018).  $L_b$  is measured through laser-induced fluorescence (LIF) (Charalampous *et al.* 2009a,b) or is estimated photographically (Jiang *et al.* 2019; Sridhara and Raghunandan 2010). There are several prediction equations for  $L_b$  presented in literature based on experimental investigations (Broumand *et al.* 2017; Engelbert *et al.* 1995; Eroglu *et al.* 1991; Lasheras *et al.* 1998; Leroux *et al.* 2007; Porcheron *et al.* 2002). Although a satisfactory agreement with the specific experimental data is demonstrated in each case, these equations cannot be used for the prediction of other spraying configurations.

It is notable that, except for the initial conditions, the air resistance on water droplets also affects the accuracy of the trajectory prediction model. There are various empirical air resistance models presented in literature (Lorenzini 2004). Li and Kawano (1995) analyzed the influence of the shape of orifice on the air resistance faced by the droplets and proposed an air resistance model suitable for non-circular nozzles. Zhu *et al.* (2019) compensated the computing error based on the method of double function difference compensation and corrected the air resistance coefficient through experimental results for accurately predicting the jet trajectory. Recently, Qu *et al.* (2021) and Shang *et al.* (2021) proposed an air resistance model based on the changes in the cross-sectional area of the water jet during flight. This technique provides a new approach for modeling the influence of air resistance on the jet falling position. For the water droplets with diameters ranging from 0-5 mm, Yan *et al.* (2010) compared 5 air resistance models and proved that the models proposed by Park and Fukui have a better accuracy.

In this work, we present a modified model for predicting the motion of sprayed water droplets and the resulting precipitation. We implement the models for the jet breakup length and droplet secondary breakup based on the classical trajectory model. Contrary to the models that assume uniform diameter of droplets, in the proposed model, we consider the droplets with different diameters and velocities. The accuracy of the proposed model is evaluated based on the water application rate of a sprinkler. The proposed modifications improve the prediction accuracy of the model and are suitable for the water trajectory prediction of non-atomizing sprinkler.

## 2. MATERIALS AND METHODS

### 2.1 Model Development of the Water Droplets Movement

The magnitude and direction of external forces on water droplets determine their motion after the jet's

fragmentation. In addition to gravity, air resistance is another major external force. The average diameter of sprinkler irrigation droplets is small, so the air resistance on the droplets is mainly inertial resistance. The inertial resistance  $F$  is calculated using the Stokes resistance equation (Carrion *et al.* 2001):

$$F = \frac{C_d \rho_a V^2 A}{2} \quad (1)$$

where,  $A$  denotes the characteristic cross-section of the droplet ( $m^2$ ),  $\rho_a$  denotes the air density ( $kg\ m^{-3}$ ), and  $V$  denotes the resultant velocity of the water droplet ( $m\ s^{-1}$ ).  $C_d$  represents the coefficient of air resistance, which is highly correlated with the Reynold number ( $Re$ ). The motion model of a three-dimensional water droplet is mathematically expressed as follows (De Lima *et al.* 2002):

$$\begin{cases} \frac{du_x}{dt} = -\frac{3}{8} \frac{C_d \rho_a}{R \rho_w} \sqrt{u_x^2 + u_y^2 + u_z^2} \cdot u_x \\ \frac{du_y}{dt} = -\frac{3}{8} \frac{C_d \rho_a}{R \rho_w} \sqrt{u_x^2 + u_y^2 + u_z^2} \cdot u_y \\ \frac{du_z}{dt} = -\frac{3}{8} \frac{C_d \rho_a}{R \rho_w} \sqrt{u_x^2 + u_y^2 + u_z^2} \cdot u_z + \frac{\rho_a - \rho_w}{\rho_w} g \end{cases} \quad (2)$$

where,  $u_x$ ,  $u_y$  and  $u_z$  are the velocity components in the  $x$ ,  $y$  and  $z$  direction ( $m\ s^{-1}$ ), respectively.  $R$  is the radius of the water droplet ( $m$ ),  $\rho_w$  is the density of water ( $kg\ m^{-3}$ ),  $g$  is the gravitational acceleration in  $9.81\ (m\ s^{-2})$ . The fourth-order Runge-Kutta method is employed for obtaining the iterative solution of the aforementioned equations, at a time step  $\Delta t$  of  $0.001\ s$ . In the proposed model,  $C_d$  is calculated based on the model presented by Fukui *et al.* (1980):

$$C_d = \begin{cases} \frac{33.3}{Re} - 0.0033Re + 1.2 & (Re \leq 128) \\ \frac{72.7}{Re} - 0.000056Re + 0.48 & (128 < Re < 1440) \\ 0.45 & (Re \geq 1440) \end{cases} \quad (3)$$

$$Re = \frac{Vd}{\nu} = \frac{2\sqrt{u_x^2 + u_y^2 + u_z^2}R}{\nu} \quad (4)$$

where,  $\nu$  is the dynamic viscosity of air ( $m^2\ s$ ), and  $d$  is the diameter of water droplets ( $m$ ).

## 2.2 Model Initial Conditions

The breakup regime of liquid jet from the irrigation sprinkler is the second wind-induced regime, which means the fluctuations on the jet surface start from the orifice and the secondary droplets breakup exists during the spraying process (Hua *et al.* 2021). Figure 1 presents a two-dimensional schematic diagram of a sprinkler jet flow and spraying process. After ejection from the nozzle, the water jet breaks from a

continuous water column into several drops under the combined action of internal velocity gradient and the surface tension of the cylindrical jet. This process is known as the primary jet breakup. The length of the water column section is the jet breakup length ( $L_b$ ). At primary breakup position, the water droplets have different diameters and velocities, which cause them to follow different flight trajectories. Afterwards, many of these droplets further breakup into multiple sub-droplets, due to the surface tension and air resistance. This process is known as the secondary droplets breakup. These droplets travel in a parabolic trajectory and fall on the ground to irrigate the target area. The landing position of the droplets is mainly influenced by three initial conditions, namely  $L_b$ , the droplet diameter distribution, and the secondary breakup behavior. Therefore, the detailed theoretical derivation of the proposed model focuses on these three conditions.

### 2.2.1 Jet Breakup Length $L_b$

The jet breakup length is the distance from the nozzle orifice to the initial fragmentation position of the water jet, which is considerably influenced by the structure of the sprinkler. The specific value of  $L_b$  is obtained by performing experiments. According to the experimental research of Jiang (2019), which studied the same type of sprinkler considered in this work (in Fig. 4a), the relationship between  $L_b$  and the diameter of the nozzle orifice is expressed as follows:

$$\frac{L_b}{D} = 23.072 \left(\frac{H}{D}\right)^{0.1751} \quad (5)$$

where,  $H$  is pressure, expressed in meters of water ( $m$ ), and  $D$  is the diameter of the orifice ( $m$ ).

### 2.2.2 Initial Water Droplet Group

In order to address the sprinkler precipitation problem using the proposed model, the required initial parameters associated with the group of water droplets include the initial droplet velocities, the initial droplet diameters, and the number of droplets.

The number of droplets can be estimated from the flowrate of the sprinkler. Let the flowrate of the sprinkler be  $Q$  ( $mm^3\ h^{-1}$ ), which represents the amount of water sprayed in a full circle. We assume that when the sprinkler is fixed, the spread angle of the irrigated area is about  $2^\circ$ . The water volume in this radial direction per unit time is calculated as:

$$X = \frac{2Q}{360} \quad (6)$$

We denote the water volume of the sprinkler in the model as  $X$  ( $mm^3\ h^{-1}$ ). The number of all water droplets  $N$  is calculated by considering the average

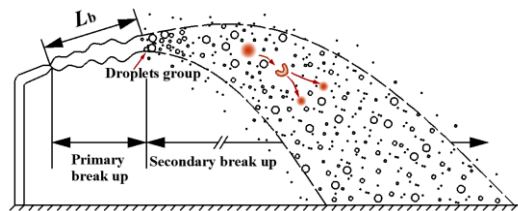


Fig. 1. A two-dimensional schematic diagram of sprinkler jet and spraying process.

droplet diameter  $\bar{d}$  (mm) and spraying time  $t$  (s), as shown in Eq. (7):

$$N = \frac{Xt}{3600 \frac{4}{3} \pi (\frac{\bar{d}}{2})^3} \quad (7)$$

The spraying time is adjustable for different spraying problems. In this model,  $t$  is set to 20 seconds. The average diameter of a water droplet is obtained based on the experimental measurements. In this model,  $\bar{d}$  is measured by a two-dimensional video disdrometer (2 DVD), and the specific value is 1.63 mm for a pressure level of 200 kPa and 1.38 mm for 300 kPa. After calculating  $N$ , we test the model's dependence on the number of droplets to ensure that the model's output remains reasonable regardless of  $N$ .

In this model, we assume that the diameter distribution of the group of water droplets at the primary breakup position conforms to the Rosin-Rammler function (Bailey *et al.* 1983; Park *et al.* 2005). The probability density function of this distribution is:

$$Y_d = e^{-\left(\frac{d}{d_c}\right)^n} \in (0,1) \quad (8)$$

$$d_c = k_1 d_{32} \left(1 - \frac{1}{n}\right)^n \quad (9)$$

$$d_{32} = k_2 \lambda We^{-0.74} \quad (10)$$

$$We = \frac{\rho_w V^2 \lambda}{\sigma} = \frac{\rho_w V^2 d_c}{8\sigma} \quad (11)$$

where,  $Y_d$  is the fraction of the total volume contained in the droplets of diameter less than  $d$ .  $n$  is the scattering coefficient (set as 3.5 in this work), which affects the range of droplet size distribution.  $d_c$  (Lefebvre and McDonell 1988) is the characteristic droplet size (m), which is obtained by using the Sauter mean droplet diameter (Wu *et al.* 1992)  $d_{32}$  (m).  $\lambda$  is the radial integral length scale at the orifice based on the equivalent diameter of nozzle orifice  $d_c$  (m). The nozzle orifice diameter is 5 mm.  $We$  is the Weber number and  $\sigma$  is the surface tension coefficient of water (N m<sup>-1</sup>). Since the Eq. (9) and Eq. (10) are typically obtained by testing the spray nozzles, we added correction coefficients  $k_1$ (1.3) and  $k_2$ (332.5) in the formulas to obtain a reasonable diameter distribution of droplets for irrigation jets.

In this model, we assume that the velocity of a water droplet group at the primary breakup position conforms to the Gamma distribution (Jones and Watkins 2012):

$$\begin{cases} f(V_0) = \frac{V_0^{a-1}}{b^a \Gamma(a)} e^{-\frac{V_0}{b}} \\ \Gamma(a) = \int_0^\infty \frac{V_0^{a-1}}{b^a} e^{-\frac{V_0}{b}} dV_0 \\ a = 0.25 V_0 = 0.25 \sqrt{2gH}, b = 4 \end{cases} \quad (12)$$

where,  $f(V_0)$  denotes the probability density function of Gamma distribution,  $\Gamma(a)$  is the Gamma function,  $a$  is the shape parameter,  $b$  is the scale parameter, and  $V_0$  is the initial velocity of the drops (m s<sup>-1</sup>).

### 2.2.3 Secondary Droplets Breakup

As mentioned previously, a secondary breakup occurs when the drops further break apart due to aerodynamic drag (Jain *et al.* 2019). The analysis of the force on the drops shows that a drop breaks when  $We$  is greater than the surface tension. The secondary breakup occurs when the velocity of a drop is greater than a critical velocity  $V_c$  (m s<sup>-1</sup>), and expressed as Eq. (13):

$$V_c = \sqrt{\frac{8\sigma}{C_{d\rho_a d}}} \quad (13)$$

In order to obtain the flight trajectory of the final sub-droplet, the new radius and velocity of the sub-droplet after secondary breakup should be computed. According to the wave breaking model proposed by Liu *et al.* (1993), the breaking of the liquid column is caused by the fluctuations caused by the relative velocity between gas and liquid. The maximum growth rate  $\Omega$  and corresponding wavelength  $\Lambda$  of an unstable surface wave are used to determine the breaking time  $\tau$  (s) and the radius of the sub-droplet  $r$  (m). The rate of the change of the drops' radius  $R$  (m) is expressed as follows:

$$\begin{cases} \frac{dR}{dt} = -\frac{R-r}{\tau} \\ r = 0.61\Lambda \end{cases} \quad (14)$$

The breaking time  $\tau$  is mathematically expressed as:

$$\tau = \frac{3.726B_1 R}{\Lambda \Omega} \quad (15)$$

where,  $B_1$  is an empirical coefficient, which is set to 1.73 in this work,  $\Lambda$  represents wavelength of rapidly growing Kelvin-Helmholtz unstable waves, and  $\Omega$  denotes the maximum growth rate of the unstable surface waves. They are mathematically expressed as follows:

$$\Lambda = 9.02 \cdot \frac{(1+0.45Oh^{0.5})(1+0.4T)^{0.7} R}{(1+0.87We_w^{1.5})^{0.6}} \quad (16)$$

$$\Omega = \frac{\left(\frac{\sigma}{\rho_w R^3}\right)^{0.5} (0.34+0.38We_w^{1.5})}{(1+Oh)(1+0.4T^{0.6})} \quad (17)$$

$$Oh = \frac{We_w^{0.5}}{Re} \quad (18)$$

$$T = Oh \cdot We_a^{0.5} \quad (19)$$

where,  $We_w$  is the Weber number of water, and  $We_a$  is the Weber number of air at room temperature.

### 2.3 Theoretical Calculation of the Water Application Rate

We use the water application rate for quantitative verification of the proposed model. Fig. 2 presents a schematic diagram of the computation process of the sprinkler water distribution in the  $x$ - $y$  plane, which represents the ground. The sprinkler is fixed at point  $O$  and sprays in the diagonal direction. The volume of water along the radial direction on the ground ( $z = 0$ ) is calculated in cumulative iterations. The computation steps are presented below.

Step 1: Based on the wetting radius of the sprinkler

considered in this study, the target irrigation region is a square with a side length of 15 m.

Step 2: To ensure the computation efficiency, the sub area for calculating the volume of droplets at each step is a square with a side length of 0.3 m. As shown in Fig. 2, after computing the volume of droplets, the target square is moved by 0.1 m in the horizontal and in the vertical direction.

Step 3: Repeat the above steps until the two-dimensional target region (15 × 15 m<sup>2</sup>) is entirely covered. The radial water application of the sprinkler is obtained based on the cumulative calculation of the volume of water in the swept area. The water application rate  $I$  (mm h<sup>-1</sup>) of the sprinkler in every grid tile is calculated using Eq. (20).

$$I = \frac{\sum_3^4 \pi R^3}{(0.1 \times 1000)^2 \times t} = \frac{\sum_3^4 \pi R^3}{10000 \times \frac{20}{3600}} = \frac{9 \sum_3^4 \pi R^3}{500} \quad (20)$$

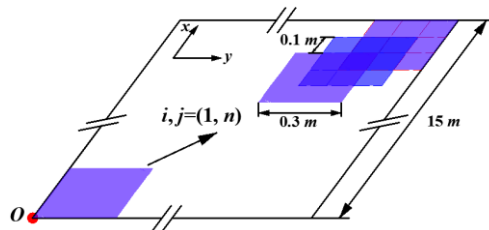


Fig. 2. A schematic diagram for calculating water application rate  $I$  in the  $x$ - $y$  plane.

The output value of the model is the volume of water along one spraying direction. The water application rate of the sprinkler is the water volume distribution in the full circular spraying area and is obtained by considering the completion of a full circle of the model's results. Thus, the results of the model can be regarded as the water application rate of the sprinkler.

We use MATLAB for the implementation of the proposed model. The workflow of the proposed method is presented in Fig. 3. As shown in Table 1, in order to illustrate the optimization of the spraying model with respect to the initial conditions of a group of droplets, four sub-models are set up for performing comparative analysis to evaluate the contribution of each of the two proposed improvements, i.e., the determination of  $L_b$  and the consideration of the secondary breakup process.

### 2.4 Experimental Setup and Procedure

We perform two experiments to validate the correct implementation of the proposed model. First, a hydraulic experiment is performed to compute the water application rate. Second, a measurement of droplet characteristics using a two-dimensional video disdrometer (2 DVD, Joanneum Research Corp, Austria) is performed. The measured parameters include the terminal velocity and the average diameter of the droplets, which are used in Eq. (7). Table 2 presents the values of parameters used in the experiments performed in this work. The experiments are performed in the sprinkler irrigation laboratory of Jiangsu University, China, which

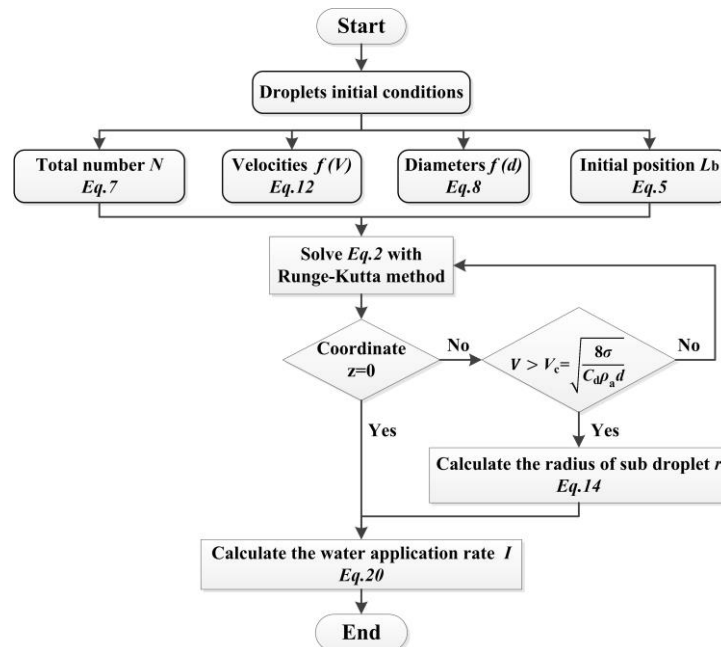


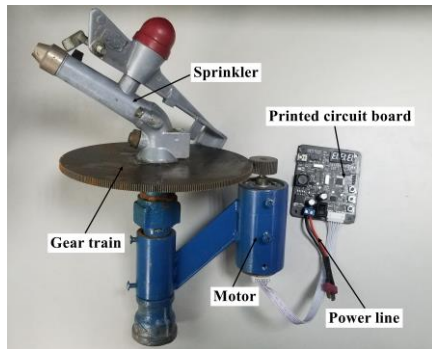
Fig. 3. Flowchart of the proposed optimized prediction model.

Table 1 Sub-model types for comparative analysis

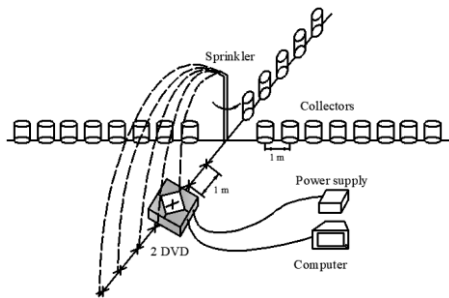
Models	Type	Description
Model 1	The proposed model	With $L_b$ and secondary breakup process
Model 2	One of the comparative models	Without $L_b$ , but with secondary breakup process
Model 3	One of the comparative models	With $L_b$ , but without secondary breakup process
Model 4	One of the comparative models	Without $L_b$ and secondary breakup process

**Table 2** Experimental parameters of the irrigation water jet

Parameters	Values	
Pressure (kPa)	200	300
Flowrate ( $\text{m}^3 \text{h}^{-1}$ )	1.414	1.732
Initial velocity ( $\text{m s}^{-1}$ )	20	24.5
Jet breakup length (m)	0.49	0.53
Number of droplets for calculation (per hour)	383880	788284



(a)



(b)

**Fig. 4. Experimental setup: (a) prototypical sprinkler rotating device and (b) schematic diagram of the experimental system.**

provides an adequate windless space. The PY15 impact sprinkler (Jinlong Spray Irrigation Co., Zhejiang, China) is used for irrigation jet spraying with a pitch angle of  $23^\circ$  at a height of 1.6 m. The resulting radius of irrigated area is about 16 m. In order to analyze the trajectory of the undisturbed jet, the influence of auxiliary nozzle and impact-driven arm is eliminated. The impact sprinkler is unable to rotate without the impact-driven arm. Therefore, a gear rotation device driven by a motor is designed to realize uniform rotation of the sprinkler, as shown in Fig. 4a. The direction of rotation and the speed of sprinkler are controlled using a circuit board, rotating clockwise at 6.5 rpm. Fig. 4b shows a schematic diagram of the experimental system. For the hydraulic experiment, the collectors are placed along 4 perpendicular radii directions and the test results are averaged to reduce the measurement error. The collectors are spaced at a distance of 1 m along each spraying line. The value of the water applied rate is directly obtained from the scale on the standard collectors. For the droplet test experiment, the measuring positions of the 2 DVD are set at 1 m intervals along the radial direction. At each test

position, more than 500 water droplets are measured, and abnormal data are eliminated based on the  $3\sigma$  criterion.

### 3. RESULTS AND ANALYSIS

#### 3.1 Experimental validation of the model

Figure 5 presents the water application rate of the sprinkler computed under two different operating pressures, along with the experimental data for comparison. The water application rate within the range of the sprinkler shows different characteristics at different locations. In order to facilitate the description and analysis, we refer to the range of 2-12 m as the “front” region and the range of 12-16 m as the “end” region. In Fig. 4a, at a pressure of 200 kPa, the water application is mainly concentrated around 12-14 m, with a peak value of  $3.27 \text{ mm h}^{-1}$ . Due to relatively low pressure, the water jet maintains its stability without too much dispersion. Therefore, the precipitation is concentrated in a small region, and there is almost no water delivered near the nozzle. The comparison of the results shows a good accuracy, especially the prediction of peak value of the water application rate and precipitation in the end region. The relative error of the water application rate between the calculated and measured results at the peak position of 13 m from the nozzle is 3.7%, and an average error of 28.7% at the end region. Even though the computed water applied rate is larger than the measured results, the average error is within 59%. Fig. 4b exhibits the same validation profile for a pressure of 300 kPa. In this case, the major volume of water is also concentrated around 12-14 m, but with a lower irrigation peak of  $2.85 \text{ mm h}^{-1}$ . The relative error of the water application rate between the computed and measured results at the peak position of 13 m from the nozzle is 5.6%, and an average error of 11.1% at the end region. The volume of water in the range of 7-10 m is greater as compared to that of 200 kPa, which is attributed to the violent turbulence and diffusion of the water jet under higher operating pressure. With the instability of the water jet, the stable core region is shortened, causing the breaking behavior to occur closer to the orifice of the sprinkler, thus resulting in higher water accumulation in the front region. Therefore, the insufficient description of the jet breakup mode under high pressure results in lower computed values of water application rate as compared to the test values, especially in the front region with an average error of about 63%. Overall, the model calculation results show good agreement with the experimental data. Even though there are some differences near the front region, the overall calculated profiles match the test data effectively.

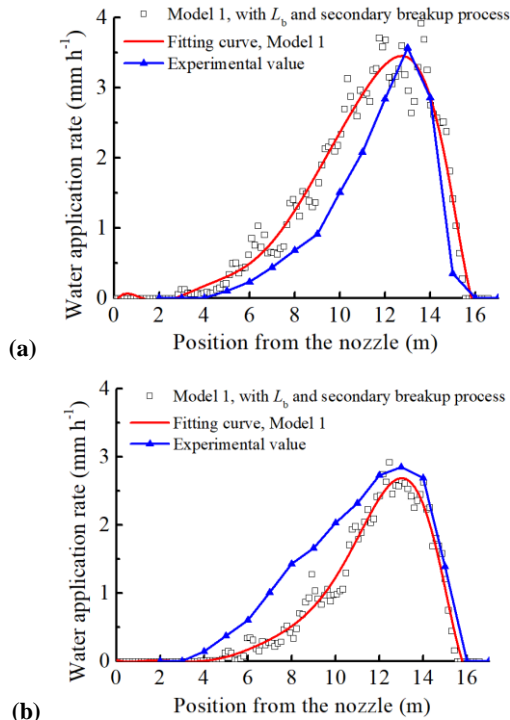


**Fig. 5. Validation of the proposed model based on the experimental data at (a) 200 and (b) 300 kPa.**

### 3.2 Verification of the Effect of Jet Breakup Length on Model

A section of the agricultural sprinkler's irrigation jet near the nozzle outlet forms a water column, thus allowing it to achieve a longer radius of the irrigated land and cover a larger field area. The length of the water column section is the jet breakup length, which affects the initial position of the water droplets. The  $L_b$  used in the proposed model is obtained by using Eq. (5). The corresponding values are provided in Table 2. Fig. 6 shows a comparison of the water application rate obtained by using the models with and without  $L_b$ . The curve fitting of the model calculation results is performed by using the least squares method. The results show that the  $L_b$  has a little effect on the prediction value of the water application rate. However, it will affect the estimated location of precipitation, especially in the regions away from the sprinkler. The peak position of the water application rate obtained by Model 1 is at 13 m, which is similar to experimentally measured location, whereas the position predicted by the Model 2 is closer to 12 m. Please note that the Model 2 refers to the model that does not consider  $L_b$ . In this model, the initial position of the droplet group is closer to the orifice. After solving the differential equation of motion, the falling positions of the droplets are also closer to the nozzle, resulting in a different distribution of water application rate as compared with real spraying. Therefore, when modelling the sprinkler spraying,  $L_b$  is an important factor that affects the prediction accuracy of location. In order to ensure the accuracy of the spraying model, the length of this water column should be considered.

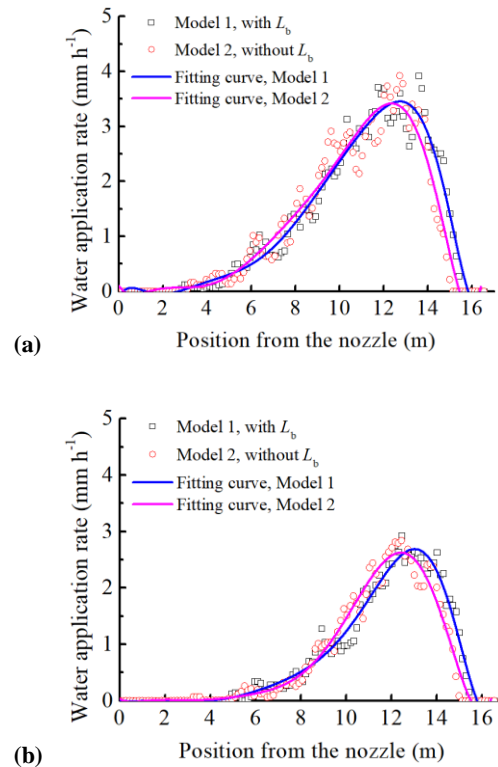
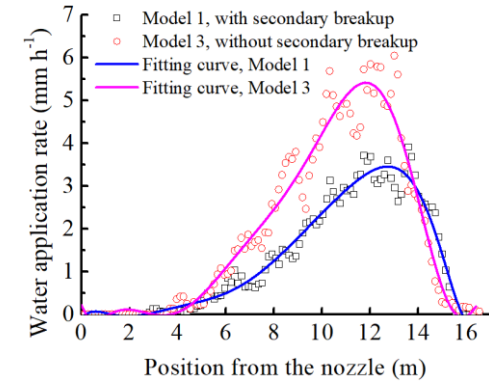


**Fig. 6. A comparison of the models with and without the  $L_b$  at (a) 200 and (b) 300 kPa.**

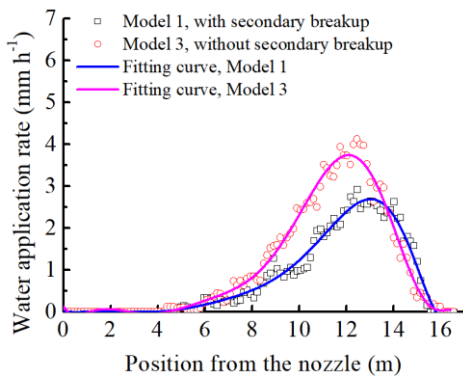
### 3.3 Verification of the Effect of Secondary Breakup Process on Model

Figure 7 presents a comparison of the results of the proposed models to validate the effect of secondary breakup. The presence of the secondary breakup process in the model has a significant effect on the computed results. Fig. 5 shows that the Model 1 accurately predicts the peak value and position of the water application rate. However, the computed results of Model 3 over predicts the water application rate with errors of 357% and 285% under 200 kPa and 300 kPa, respectively. Although, both models demonstrate errors in their predictions of water application rate along the spraying direction, Model 1 obtains a better prediction accuracy for the value and position of the water application rate at the peak position. Furthermore, the results show that the breakup process significantly affects the peak position of water application rate. Model 3 predicts the peak position 1 m closer to the sprinkler as compared to Model 1. In addition, as compared to the results of  $L_b$  presented in Fig. 6, the secondary breakup of droplets has a more significant impact on the spraying distribution estimation accuracy.

The calculated results of the spraying model with the secondary breakup process also highlight the positive relationship between the operating pressure and the jet breakup. For a pressure of 200 kPa, the proportion of water droplets that undergo a secondary breakup process is 27.1%. This proportion increases to 48.2% when the pressure is 300 kPa. Therefore, more droplets undergo the secondary breakup process at a higher pressure and form a larger range of smaller water droplets with different



(a)



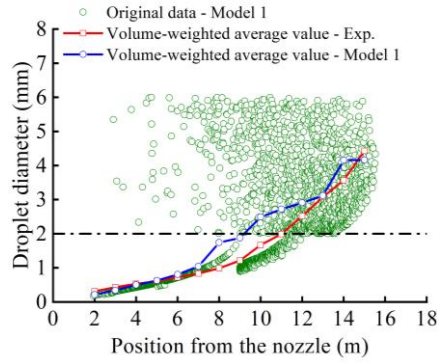
(b)

**Fig. 7. A comparison of the models with and without secondary breakup process at (a) 200 and (b) 300 kPa.**

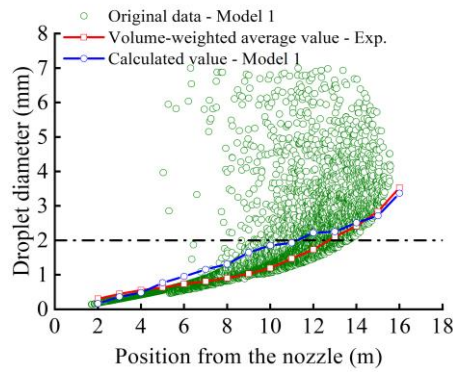
diameters and velocities. These droplets fall at different positions along the spraying direction to form uniform precipitation, which explains the improvement in spraying performance at higher pressures.

### 3.4 Analysis of the Diameter and Terminal Velocity of Droplets

Figure 8 shows the distribution of the droplets' diameters at different positions from the nozzle calculated using Model 1 and is compared with the experimental values. The  $3\sigma$  criterion is used to eliminate the abnormal data for obtaining the volume-weighted average diameter of the water droplets. It is evident from Fig. 8 that the average diameter of droplets increases with an increase in the distance from the nozzle. At the front spraying range, the average diameter of the droplets ranges from 0-2 mm. The Model 1 matches the experimental measurements effectively. At 200 kPa, the water jet remains concentrated in the range of 2-10 m, and the spraying droplets in this region are small, i.e., diameters concentrated within 2 mm. In the range of 11-16 m, under the dispersion effect of the jet, the water droplet group comprises many droplets with different diameters, ranging from 2-6 mm. Since the provided experimental data contains the volume-weighted average values, the data lies among the values predicted by the Model 1. The corresponding phenomenon at 300 kPa is shown in Fig. 8b. Due to the increased proportion of secondary breakup of the



(a)



(b)

**Fig. 8. A comparison between the volume-weighted average droplets' diameters obtained from experiment and Model 1 at (a) 200 and (b) 300 kPa.**

droplets, more small droplets are concentrated along the spraying direction. Therefore, the calculation results are more consistent with the experimental values. Overall, Fig. 8 shows that Model 1 is able to predict the diameter of the sprayed droplets accurately.

Figure 9 shows the predictions and experimental data of the terminal velocities of droplets at operating pressures of 200 kPa and 300 kPa. The terminal velocities of droplets along the spraying direction are measured by using the 2 DVD equipment. Due to the measuring accuracy of the equipment, the largest diameter of the droplet that is accurately measured is 5 mm. It is evident from the experimental results that the terminal velocity and droplet diameter are positively correlated. The relationship between the velocity and diameter of droplets obtained using the proposed model shows a similar positive correlation with the experimental results. However, the computed values of the terminal velocities are larger as compared to the corresponding measured values. This is caused by the air resistance on the droplets. This means that a more accurate air resistance model is required to estimate the experimental values more accurately. As presented in Fig. 9, as compared with Model 4, the modified Model 1 has the ability to calculate the movement of sub-droplets with a diameter of less than 2 mm, which has proved to be very important for the spraying distribution presented in Fig. 8. Thus, Model 1 improves the

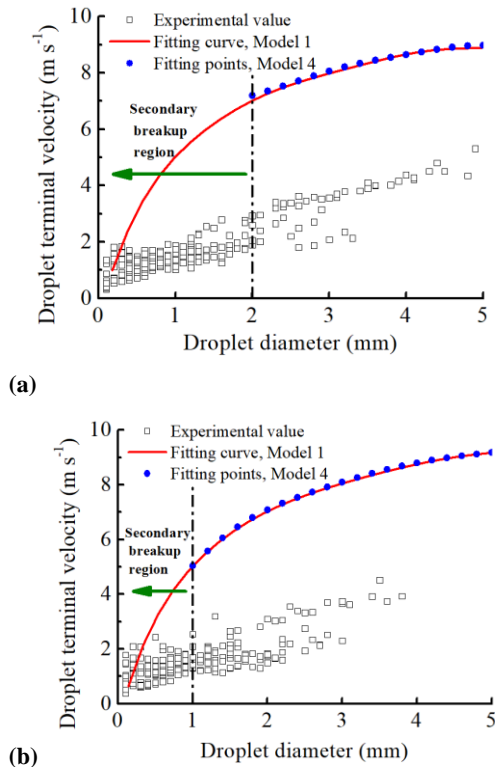


**Fig. 9. Relationship between the diameter and velocity of droplets obtained using the presented model and experimental results at (a) 200 and (b) 300 kPa.**

accuracy of precipitation estimation based on the secondary breakup process of water droplets.

#### 4. DISCUSSION

In this work, we established a three-dimensional sprinkler spraying prediction model based on jet breakup theory and the droplet movement equation. The secondary breakup process of droplets and jet breakup length ( $L_b$ ) are considered in the proposed model to improve the prediction accuracy. In this spraying model, the secondary breakup of droplets occurs as follows: when the velocity and diameter of a large water drop conform to the critical secondary breakup condition presented in Eq. (13), the drop splits into two sub-droplets and smaller new drops are formed. The effect of air resistance on the sub-droplet becomes more significant as the diameter of the sub-droplet decreases from its original size rapidly. Due to this effect, the sub-droplets deviate quickly from the original trajectory. During the falling process, the sub-droplets slow down due to the continuous drag force, until they reach the ground. The landing point of the sub-droplet is closer to the nozzle than that of the original drop. In other words, the existence of sub-droplets mainly results in precipitation near the nozzle. At the same time, the new main droplets formed after the secondary breakup retain most of the mass of the original drops. Although the diameters have not changed substantially, the velocities are reduced. Therefore, most of the new main drops no longer meet the

conditions for the secondary breakup until they reach the ground. These droplets mainly increase the water application rate of the end region.

We observe that the prediction results using the mathematical models still have calculation errors between the predicted water application rate and the experimental values, especially among the front range of the wetting radius. A possible reason for this phenomenon is that there are differences between the initial conditions of the water droplets in the mathematical models and the actual jet broken droplets. These differences deteriorate the accuracy of the model. However, in the proposed model, the wave breaking model (Liu *et al.* 1993) is used to predict the secondary breakup of the water droplets, which describes the spraying process of the water jet accurately. The water droplet fragmentation modes are divided into low-speed and high-speed modes. The Rayleigh-Taylor instability occurs at low-speed mode and produces a new droplet with a large diameter, while the growth of the Kelvin Helmholtz instability wave at high-speed mode produces a new droplet with a much smaller diameter. In the wave breaking model, the small droplets are sheared from the jet surface due to the relative velocity gradient and the growth of the Kelvin Helmholtz instability wave. The irrigation water jet in this work operates in the high-speed mode. Thus, the wave breaking model effectively describes the breaking behavior of the irrigation water jet in this work. In fact, the results show a good agreement between the water application rate peak predicted by the proposed model and the experimental values. The errors of the peak value of the water application rate between the computed result of the presented model and the experimental data are 3.7% under 200 kPa, and 5.6% under 300 kPa. The so-called liquid jet breakup length, also called the liquid core length, is the axial location where the continuity of the liquid jet is interrupted.  $L_b$  depends on the primary breakup of the liquid jet, which is strongly affected by the geometry of the sprinkler. In the proposed model,  $L_b$  is obtained by using a semi-empirical formula based on test measurement which is only applicable to the specific sprinkler in this work. In order to apply the proposed model to other configurations, a universal equation for breakup length should be devised. A more applicable equation for predicting the breakup length of the irrigation jet, comprehensive analysis combining numerical simulation, theoretical analysis, and experimental validation will be considered in future research.

Except the secondary breakup of droplets and the  $L_b$ , the air resistance coefficient is also an important parameter that affects the prediction accuracy of the spraying model (Yan *et al.* 2010). The external factors that affect the air resistance coefficient include the relative velocity between wind and droplets, the shape and size of the droplets, Reynolds number, etc. When modelling a specific spraying problem, in order to calculate the movement state of water droplets more accurately, a correction coefficient of the air resistance equation, which is obtained by using at least one set of test data is suggested. Furthermore, the modified spraying prediction model presented in this work is only applicable for spraying in a windless environment. In order to apply the model to predict actual irrigation

spraying efficiency in farmlands, an extended model that considers the influence of the wind and ambient temperature, based on the model presented in this work needs to be established.

## 5. CONCLUSIONS

In this work, the water droplet trajectory of an irrigation sprinkler is analyzed and modelled. The trajectory and droplet movement equations are established according to the particle kinematics and jet fragmentation theory. Based on the characteristics of liquid jet fragmentation, special consideration is paid to the effects of the secondary breakup of droplets and the jet breakup length. This improves the prediction accuracy of the model. The main conclusions of this work are presented below.

- (1) The output value of the proposed model is the water applied rate of the sprinkler, which is in good agreement with the experimental data. The relative error in the peak value is less than 6%. The effect of the secondary breakup of droplets on the model accuracy is more significant than  $L_b$ .
- (2) The amount of the secondary breakup of droplets is proportional to pressure. The reason for the improvement in the accuracy of the proposed model is the calculation of the sub-droplets smaller than 2 mm. These small droplets considerably affect the formation of water applied rate of the sprinkler.
- (3) The proposed model can be applied to sprinkler irrigation jets under various working conditions. Once the flowrate and the initial velocity of the irrigation jet have been determined, the trajectory and distribution of water droplets can be predicted. For different types of sprinklers and operating conditions, the applicability and accuracy of the spraying prediction model can be improved by adjusting the key parameters.

## ACKNOWLEDGEMENTS

This work was supported by the National Natural Science Foundation of China (grant numbers No.51939005, No.51809119), the Graduate Research and Innovation Projects of Jiangsu Province (grant number KYCX21\_3345).

## REFERENCES

- Aghajani, H., S. Dembele and J. X. Wen (2014). Analysis of a semi-empirical sprinkler spray model. *Fire Safety Journal* 64, 1–11.
- Ashgriz, N. and J. Y. Poo (1990). Coalescence and separation in binary collisions of liquid drops. *Journal of Fluid Mechanics* 221, 183–204.
- Bailey, A. G., W. Balachandran and T. J. Williams (1983). The rosin-rammler size distribution for liquid droplet ensembles. *Journal of Aerosol Science* 14(1), 39–46.
- Broumand, M., G. Rigby and M. Birouk (2017). Effect of Nozzle Exit Turbulence on the Column Trajectory and Breakup Location of a Transverse Liquid Jet in a Gaseous Flow. *Flow, Turbulence and Combustion* 99(1), 153–171.
- Carrión, P., J. M. Tarjuelo J. and Montero (2001). SIRIAS: A simulation model for sprinkler irrigation. I. Description of model. *Irrigation Science* 20(2), 73–84.
- Charalampous, G., Y. Hardalupas and A. Taylor (2009a). Structure of the Continuous Liquid Jet Core during Coaxial Air-Blast Atomisation. *International Journal of Spray and Combustion Dynamics* 1(4), 389–415.
- Charalampous, G., Y. Hardalupas and A. M. K. P. Taylor (2009b). Novel technique for measurements of continuous liquid jet core in an atomizer. *AIAA Journal* 47(11), 2605–2615.
- De Lima, J. L. M. P., P. J. J. F. Torfs and V. P. Singh (2002). A mathematical model for evaluating the effect of wind on downward-spraying rainfall simulators. *Catena* 46(4), 221–241.
- Engelbert, C., Y. Hardalupas and J. H. Whitelaw (1995). Breakup phenomena in coaxial airblast atomizers. *Proceedings of the Royal Society A: Mathematical, Physical and Engineering Sciences* 451(1941), 189–229.
- Eroglu, H., N. Chigier and Z. Farago (1991). Coaxial atomizer liquid intact lengths. *Physics of Fluids A: Fluid Dynamics* 3(2), 303–308.
- Fukui, Y., K. Nakanishi and S. Okamura (1980). Computer evaluation of sprinkler irrigation uniformity. *Irrigation Science* 2(1), 23–32.
- Hua, L., H. Li and Y. Jiang (2021). Axis-switching Behavior of Liquid Jets Issued From Non-circular Nozzles under Low-intermediate Pressure. *Applied Engineering in Agriculture ASABE* 37(2), 367–378.
- Jain, S. S., N. Tyagi, R. S. Prakash, R. V. Ravikrishna and G. Tomar (2019). Secondary breakup of drops at moderate Weber numbers: Effect of Density ratio and Reynolds number. *International Journal of Multiphase Flow* 117, 25–41.
- Jiang, Y., H. Li, C. Chen and Q. Xiang (2018). Calculation and verification of formula for the range of sprinklers based on jet breakup length. *International Journal of Agricultural and Biological Engineering* 11(1), 49–57.
- Jiang, Y., H. Li, L. Hua, D. M. Zhang and Z. Issaka (2019). Experimental Study on Jet Breakup Morphologies and Jet Characteristic Parameters of Non-circular Nozzles Under Low-intermediate Pressures. *Applied Engineering in Agriculture ASABE* 35(1879), 617–632.
- Jones, D. P. and A. P. Watkins (2012). Droplet size and velocity distributions for spray modelling. *Journal of Computational Physics* 231(2), 676–692.

- Kincaid, D. C., K. H. Solomon and J. C. Oliphant (1996). Drop size distributions for irrigation sprinklers. *Transactions of the American Society of Agricultural Engineers* 39(3), 839–845.
- Lasheras, J. C., E. Villermaux and E. J. Hopfinger (1998). Breakup and atomization of a round water jet by a high-speed annular air jet. *Journal of Fluid Mechanics* 357, 351–379.
- Lefebvre, A. H. and V. G. McDonell (1988). *Atomization and sprays*. Hemisphere Publishing Corporation.
- Leroux, B., O. Delabroy and F. Lacas (2007). Experimental study of coaxial atomizers scaling. Part I: Dense core zone. *Atomization and Sprays* 17(5), 381–407.
- Li, J. and H. Kawano (1995). Simulating Water-Drop Movement from Noncircular Sprinkler Nozzles. *Journal of Irrigation and Drainage Engineering* 121(2), 152–158.
- Li, J., H. Kawano and K. Yu (1994). Droplet Size Distributions From Different Shaped Sprinkler Nozzles. *Transactions of the ASAE* 37(6), 1871–1878.
- Lin, S. P. (1996). Regimes of Jet Breakup and Breakup Mechanisms (Mathematical Aspects). In *Recent Advances in Spray Combustion: Spray Atomization and Drop Burning Phenomena* (pp. 137–160).
- Liu, A. B., D. Mather and R. D. Reitz (1993). Modeling the effects of drop drag and breakup on fuel sprays. *SAE Technical Papers* 1(1), 1–13.
- Lorenzini, G. (2004). Simplified Modelling of Sprinkler Droplet Dynamics. *Biosystems Engineering* 87(1), 1–11.
- Mugele, R. A. and H. D. Evans (1951). Droplet Size Distribution in Sprays. *Industrial and Engineering Chemistry* 43(6), 1317–1323.
- Munnannur, A. and R. D. Reitz (2007). A new predictive model for fragmenting and non-fragmenting binary droplet collisions. *International Journal of Multiphase Flow* 33(8), 873–896.
- Park, H., S. S. Yoon and S. D. Heister (2005). A nonlinear atomization model for computation of drop size distributions and spray simulations. *International Journal for Numerical Methods in Fluids* 48(11), 1219–1240.
- Porcheron, E., J. L. Carreau, L. Prevost, D. Le Visage and F. Roger (2002). Effect of injection gas density on coaxial liquid jet atomization. *Atomization and Sprays* 12, 209–227.
- Qu, Y., X. Liu, M. Zhang, Y. Wang and C. Liu (2021). Analysis and evaluation of drop point for water jet based on wave model. *Journal of Engineering Research* 9(1), 229–246.
- Shang, W., X. Liu, M. Zhang, Y. Qu and Y. Wang (2021). Firewater monitor trajectories based on jet expansion and dynamic breakup model. *Journal of Testing and Evaluation* 49(1), 435–451.
- Sridhara, S. N. and B. N. Raghunandan (2010). Photographic investigations of jet disintegration in airblast sprays. *Journal of Applied Fluid Mechanics* 3(2), 111–123.
- Wu, P. K., L. K. Tseng and G. M. Faeth (1992). Primary breakup in gas/liquid mixing layers for turbulent liquids. *Atomization and Sprays* 1(3).
- Wu, Y., L. Wang, W. Lin, G. Song, Y. He, X. Wu and K. Cen (2020). Picosecond pulsed digital off-axis holography for near-nozzle droplet size and 3D distribution measurement of a swirl kerosene spray. *Fuel* 283, 119–124.
- Yan, H. J., G. Bai, J. Q. He and Y. J. Li (2010). Model of droplet dynamics and evaporation for sprinkler irrigation. *Biosystems Engineering* 106(4), 440–447.
- Zhang, Y., D. Zhu, L. Zhang and X. Gong (2015). Water Distribution Model of Fixed Spray Plate Sprinkler Based on Ballistic Trajectory Equation. *Transactions of the Chinese Society for Agricultural Machinery* 46(12), 55–61.
- Zhu, J., W. Li, D. Lin and G. Zhao (2019). Study on Water Jet Trajectory Model of Fire Monitor Based on Simulation and Experiment. *Fire Technology* 55(3), 773–787.